JACC: BASIC TO TRANSLATIONAL SCIENCE VOL. 8, NO. 3, 2023

ORIGINAL RESEARCH - PRECLINICAL

Beneficial Effects of Low-Intensity Pulsed Ultrasound Therapy on Right Ventricular Dysfunction in Animal Models

Takashi Nakata, MD,[a] Tomohiko Shindo, MD, PhD,[a] Kenta Ito, MD, PhD,[a] Kumiko Eguchi, MD, PhD,[a] Yuto Monma, MD, PhD,[a] Sadamitsu Ichijo, MD, PhD,[a] Rie Ryoke, PhD,[b] Wakako Satoh, BA,[c] Kazunori Kumasaka, BA,[c] Haruka Sato, MD, PhD,[c] Ryo Kurosawa, MD, PhD,[a] Kimio Satoh, MD, PhD,[a] Ryuta Kawashima, MD, PhD,[b] Masahito Miura, MD, PhD,[c] Hiroshi Kanai, PhD,[d,e] Satoshi Yasuda, MD, PhD,[a] Hiroaki Shimokawa, MD, PhD[a,f]

VISUAL ABSTRACT

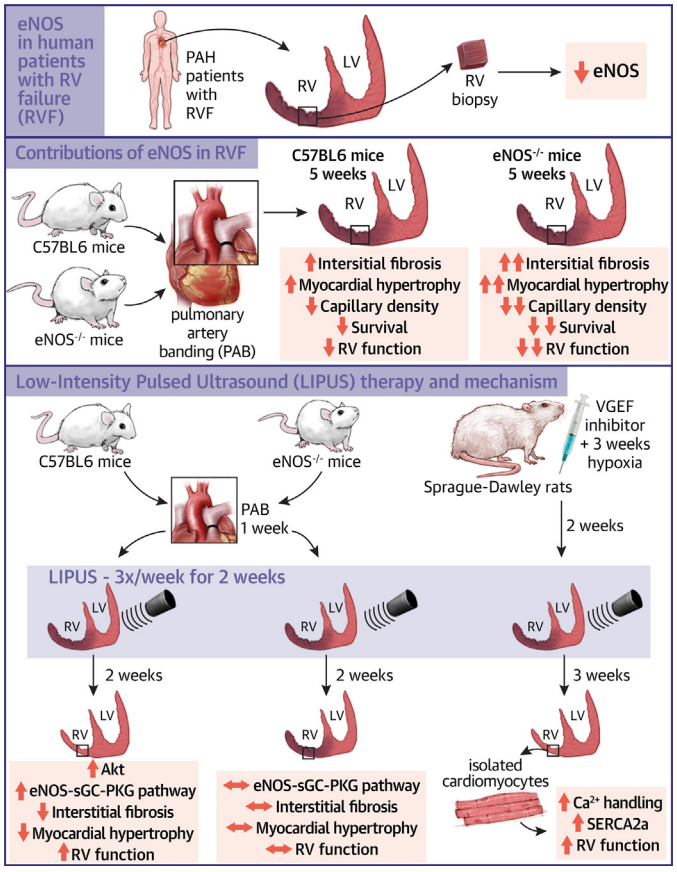

Nakata T, et al. J Am Coll Cardiol Basic Trans Science. 2023;8(3):283–297.

HIGHLIGHTS

- **eNOS is downregulated in the RV of patients with RVF.**
- **eNOS and its downstream signals are downregulated in a mouse model of PAB and a rat model of RVF with Sugen/hypoxia.**
- **eNOS$^{-/-}$ mice show the worsening of RV function compared with WT mice after the PAB procedure.**
- **LIPUS therapy ameliorates RV dysfunction in both animal models associated with activation of eNOS.**
- **The beneficial effects of LIPUS therapy are absent in eNOS$^{-/-}$ mice.**
- **LIPUS therapy may be a possible, novel, and nonpharmacologic therapy for RVF through eNOS activation.**

ISSN 2452-302X https://doi.org/10.1016/j.jacbts.2022.08.010

JACC: BASIC TO TRANSLATIONAL SCIENCE VOL. 8, NO. 3, 2023
MARCH 2023:283–297

ABBREVIATIONS AND ACRONYMS

$[Ca^{2+}]i$ = intracellular Ca^{2+} concentration

cGMP = cyclic guanosine monophosphate

CO = cardiac output

CMR = cardiac magnetic resonance

dP/dt = rate of rise of left ventricular pressure

eNOS = endothelial nitric oxide synthase

LIPUS = low-intensity pulsed ultrasound

LV = left ventricular

NO = nitric oxide

PAB = pulmonary arterial banding

PAH = pulmonary arterial hypertension

PKC = protein kinase C

PKG = protein kinase G

PLN = phospholamban

RV = right ventricle

RVEF = right ventricular ejection fraction

RVF = right ventricular failure

RVFAC = right ventricular fractional area change

SERCA = sarcoplasmic reticulum Ca^{2+}-ATPase

sGC = soluble guanylate cyclase

TAPSE = tricuspid annular plane systolic excursion

WT = wild type

SUMMARY

Right ventricular failure (RVF) is a leading cause of death in patients with pulmonary hypertension; however, effective treatment remains to be developed. We have developed low-intensity pulsed ultrasound therapy for cardiovascular diseases. In this study, we demonstrated that the expression of endothelial nitric oxide synthase (eNOS) in RVF patients was downregulated and that eNOS expression and its downstream pathway were ameliorated through eNOS activation in 2 animal models of RVF. These results indicate that eNOS is an important therapeutic target of RVF, for which low-intensity pulsed ultrasound therapy is a promising therapy for patients with RVF. (J Am Coll Cardiol Basic Trans Science 2023;8:283–297) © 2023 The Authors. Published by Elsevier on behalf of the American College of Cardiology Foundation. This is an open access article under the CC BY license (http://creativecommons.org/licenses/by/4.0/).

Right ventricular failure (RVF) is a clinical syndrome mainly caused by increased right ventricle (RV) afterload and is characterized by reduced RV ejection fraction (RVEF) and dilated RV.[1] Patients with RVF show systemic venous congestion, leading to systemic organ dysfunction and peripheral edema, the pathophysiology of which appears to be different from that of left ventricular (LV) failure.[1] RVF is one of the most important prognostic factors in patients with pulmonary arterial hypertension (PAH).[2,3] It has been reported that 5-year survival in patients with reduced RVEF (<25%) is 47.1%, whereas in those with preserved RVEF (≥25%) it is 70.5%.[4] Because the RV function of PAH patients predicts the prognosis independently of the severity of PAH, RVF itself is an important therapeutic target for PAH.[5] In addition, RVF is involved in adverse outcomes of patients with LV heart failure with preserved ejection fraction and patients who have an LV assist device implanted.[6,7] Although a number of pathogenetic factors, such as ischemia, inflammation, metabolic abnormality, and fibrosis, have been proposed for RVF,[8] the detailed mechanisms still remain to be fully elucidated. Indeed, there is an urgent need to develop a robust therapy for RVF.

We previously demonstrated that low-intensity pulsed ultrasound (LIPUS) has angiogenic and anti-inflammatory effects through its mechanotransduction mechanism, and its clinical application is widely expected as a noninvasive therapeutic option for cardiovascular diseases.[9] We previously reported that LIPUS therapy induces angiogenesis in ischemic heart tissue, ameliorating cardiac dysfunction in a porcine model of chronic myocardial ischemia[10] and a mouse model of myocardial infarction.[11] Moreover, we reported that LIPUS therapy ameliorates LV dysfunction in pressure-overloaded LV by inducing angiogenesis[12] and also diastolic dysfunction in diabetic mice with diastolic LV dysfunction through enhancement of the endothelial nitric oxide synthase (eNOS)-nitric oxide (NO)-cyclic guanosine monophosphate (cGMP)-protein kinase G (PKG) pathway.[13] eNOS is one of the 3 NOS isoforms, generating NO from L-arginine and molecular oxygen as substrates.[14] eNOS is mainly expressed in endothelial cells but also in cardiomyocytes to a lesser extent, playing a pivotal role in the regulation of vascular tone and maintenance of endothelial function.[15] Indeed, the NO signaling pathway plays an important protective role in the cardiovascular system.[16,17] NO regulates cardiovascular function through activating soluble guanylate cyclase (sGC) and its downstream stimulation of cGMP and PKG.[18] Because this NO-sGC-cGMP-PKG pathway is a

From the [a]Department of Cardiovascular Medicine, Tohoku University Graduate School of Medicine, Sendai, Japan; [b]Institute of Development, Aging and Cancer, Tohoku University Graduate School of Medicine, Sendai, Japan; [c]Department of Clinical Physiology, Health Science, Tohoku University Graduate School of Medicine, Sendai, Japan; [d]Department of Electronic Engineering, Graduate School of Engineering, Tohoku University, Sendai, Japan; [e]Division of Biomedical Measurements and Diagnostics, Graduate School of Biomedical Engineering, Tohoku University, Sendai, Japan; and the [f]International University of Health and Welfare, Narita, Japan.

The authors attest they are in compliance with human studies committees and animal welfare regulations of the authors' institutions and Food and Drug Administration guidelines, including patient consent where appropriate. For more information, visit the Author Center.

Manuscript received June 16, 2022; revised manuscript received August 17, 2022, accepted August 17, 2022.

second messenger system that mediates vasodilation and ameliorates cardiomyocyte remodeling,[19] targeting the pathway has attracted much attention as a possible therapeutic target for heart failure.[20] Although it has been reported that targeting the pathway improved cardiomyocyte hypertrophy, interstitial fibrosis, and calcium handling in pressure-overloaded LV in animals,[21,22] the role of the pathway in the pathogenesis of RVF remains to be fully elucidated.

We previously demonstrated that RV function is significantly deteriorated in eNOS-deficient ($eNOS^{-/-}$) mice when exposed to chronic hypoxia in vivo, suggesting the importance of eNOS in the pathogenesis of RVF.[23] Although several pharmacologic agents that stimulate the sGC-cGMP-PKG pathway are available for PAH patients,[24] they have systemic side effects such as hypotension because of their systemic vasodilator effect. On the other hand, our LIPUS therapy locally activates the eNOS-NO pathway in the heart, which is an advantage over pharmacologic agents. In the present study, we thus examined whether the eNOS-NO-sGC-cGMP-PKG pathway is impaired in RVF and if so, whether LIPUS therapy is effective and safe in animal models of RVF in vivo.

METHODS

A detailed description of the methods is provided in the Supplemental Appendix online.

LIPUS THERAPY. For LIPUS therapy, we used a multifunction generator (WF1974, NF Corporation Yokohama) with a bipolar amplifier (BA4825, NF Corporation Yokohama) and a planar ultrasound probe (Honda Electronics Co).[25] LIPUS therapy was performed in the following conditions: center frequency: 1.875 MHz; pulse repetition frequency: 2.74 kHz; number of cycles: 32 (17-ms burst length); spatial peak temporal average intensity: 117-162 mW/cm^2; and power of LIPUS: 0.25 MPa.[11-13] LIPUS therapy was applied to animals through an agar phantom gel, which is adjusted at a 6-cm depth where the beam of the ultrasound becomes stable.[11-13]

MOUSE MODEL OF PULMONARY ARTERY BANDING. Male wild-type (WT) mice (10 weeks old; 23 ± 28 g in body weight) were obtained from Charles Rivers Laboratories. $eNOS^{-/-}$ mice were originally provided by P. Huang (Harvard Medical School). The present mouse model of pulmonary artery banding (PAB) was previously described in detail.[26] One week after the surgery, mice in the treatment group received LIPUS therapy under general anesthesia with inhaled isoflurane (0.5%-1.0%) 3 times/week for 2 weeks. Irradiation time of LIPUS therapy was 20 minutes for 3 times (with 5-minute intervals).[11-13] Two weeks after LIPUS therapy, echocardiography and invasive hemodynamic measurements were performed, and after these examinations, they were sacrificed by blood loss.

RAT MODEL OF SUGEN/HYPOXIA-INDUCED PULMONARY HYPERTENSION. Adult male Sprague-Dawley rats weighing 180 to 220 g were purchased from Charles River Laboratories. Rats were subcutaneously injected with an inhibitor of vascular endothelial growth factor, SU5416 (Sigma) 20 mg/kg, and were exposed to hypoxia (10% O_2) for 3 weeks as previously described.[27] Two weeks after hypoxia, rats received LIPUS therapy 2 times/week for 3 weeks. Three weeks after LIPUS therapy, RV function was measured, and rats were sacrificed by blood loss.

STATISTICAL ANALYSIS. Results are shown as median (IQR). Differences between the 2 groups were analyzed using a Mann-Whitney *U* test. Data from multiple groups were analyzed using analysis of variance followed by Tukey's post hoc test for multiple pairwise comparisons for normally distributed samples with equal variances. The normality of the distributions was confirmed by the Shapiro-Wilk normality test, and the equality of the variances was tested by Bartlett's test. Pearson's correlation coefficient was used to determine the association between 2 continuous variables. Survival analysis was performed by the Kaplan-Meier method, and between-group differences in survival were tested by the log-rank (Mantel-Cox) test (GraphPad Prism [GraphPad Software Inc]). Differences with a P value of <0.05 were considered to be statistically significant.

RESULTS

eNOS EXPRESSION IN RV ENDOMYOCARDIAL BIOPSY SAMPLES OF PATIENTS WITH DILATED CARDIOMYOPATHY AND THOSE WITH PAH. The eNOS-positive area in the RV was significantly decreased in the patients with RVF vs those without it (**Figures 1A and 1B**). We also examined caveolin-1 as an endothelial cell marker and regulator of eNOS and found that the caveolin-1-positive area was comparable among the 3 groups (**Figures 1A and 1B**). There was no significant correlation between caveolin-1-positive area and eNOS-positive area (**Figure 1C**). In contrast, there was a positive correlation between eNOS expression and tricuspid annular plane systolic excursion (TAPSE)/RV fractional area change (RVFAC), but no correlation with LV function (**Figure 1D**).

IMPORTANCE OF THE eNOS-NO-sGC-cGMP-PKG SIGNALING PATHWAY IN RV DYSFUNCTION. To confirm the significance of the eNOS-NO-sGC-cGMP-

FIGURE 1 **Reduced eNOS Expression in Right Ventricular Endomyocardial Biopsy Samples From Patients With Dilated Cardiomyopathy and Those With PAH**

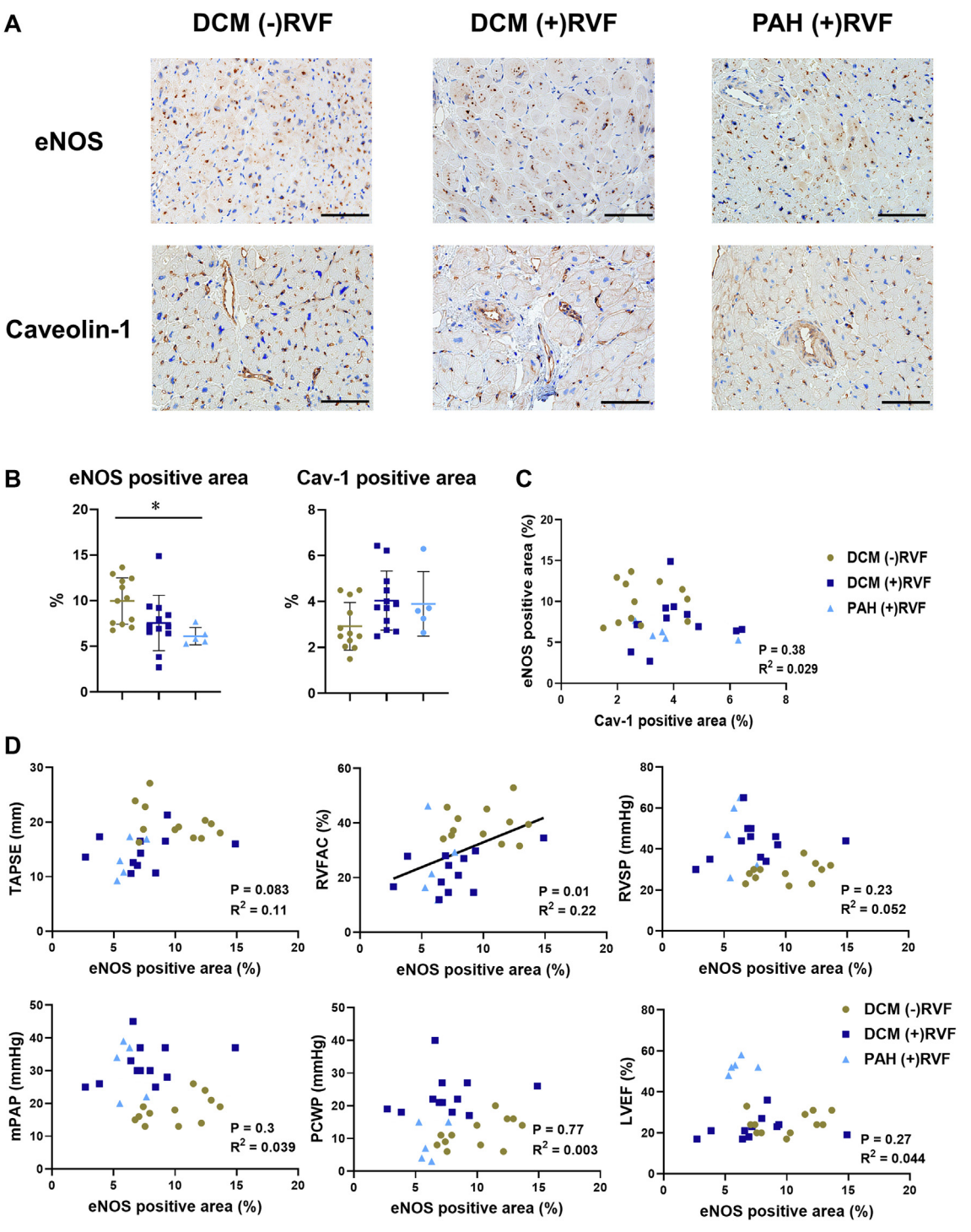

Continued on the next page

PKG signaling pathway in the pathogenesis of RVF, we first evaluated physiologic function and molecular regulation in the mouse model of PAB in vivo. One week after the PAB operation, we found that pulmonary arterial velocity was significantly increased, RV function was significantly decreased, and the RV was significantly hypertrophied and dilated compared with the sham-operated group (Supplemental Figures 1A to 1C). Although eNOS phosphorylation at Thr495 was significantly increased, that at Ser1177 was significantly decreased in PAB mice compared with sham-operated mice (Supplemental Figures 1D and 1E), indicating that eNOS activity was significantly decreased in pressure-overloaded RVs. Moreover, expression of protein kinase C (PKC) was significantly increased, and downstream signals of the eNOS-NO-sGC-cGMP-PKG pathway were also significantly decreased in PAB mice compared with sham-operated mice (Supplemental Figures 1D and 1E). Importantly, there was a strong correlation between PKC and phosphorylated eNOS at Thr495 and between phosphorylated eNOS at Ser1177 and the downstream signals (Supplemental Figure 1F). To further elucidate the importance of eNOS in RVF, we examined the effects of PAB in $eNOS^{-/-}$ mice (**Figure 2A**). $eNOS^{-/-}$ mice without PAB showed normal cardiac function in both ventricles and showed normal body weight and weights of the RV, lungs, and liver (**Figures 2C to 2F,** Supplemental Figures 2A and 2B). In contrast, in $eNOS^{-/-}$ mice with PAB, RV function and survival rate significantly worsened compared with WT mice with PAB (**Figures 2B, 2E, and 2F**). Histologic examination showed that myocardial hypertrophy was significantly increased and capillary density was significantly decreased in $eNOS^{-/-}$ PAB mice compared with WT PAB mice, whereas interstitial fibrosis was comparable between the 2 groups (**Figures 2C and 2D**). Macroscopic liver congestion was noted in $eNOS^{-/-}$ PAB mice, and liver weight was significantly higher in $eNOS^{-/-}$ PAB mice than in WT PAB mice at 5 weeks after PAB (**Figures 2C and 2D**). In the present study, although $eNOS^{-/-}$ mice showed slightly elevated blood pressure as previously reported,[28] their blood pressure was significantly decreased after PAB (Supplemental Figure 2A). In contrast, weights of the RV and lungs were comparable between WT and $eNOS^{-/-}$ mice after PAB (Supplemental Figure 2B).

LIPUS THERAPY AMELIORATES RV DYSFUNCTION IN PAB MICE. Next, we examined whether LIPUS therapy is effective for RVF in PAB mice (**Figures 3A and 3B**). Two weeks after LIPUS therapy, when pulmonary arterial velocity was comparable between the PAB-LIPUS and PAB-placebo groups, echocardiography showed that TAPSE, right ventricular dilated diameter, and cardiac index were all significantly improved in the former compared with the latter (**Figures 3C and 3D**). In contrast, there was no significant difference in body weight, blood pressure, heart rate, organ weight, or survival rate between the 2 groups (Supplemental Figures 3A to 3C). Hemodynamic evaluation showed that RV end-diastolic pressure was significantly decreased in the PAB-LIPUS group vs the PAB-placebo group and that stroke work, stroke volume, cardiac output (CO), and positive rate of rise of LV pressure (dP/dt) were significantly increased in the PAB-LIPUS group vs the PAB-placebo group (**Figures 3E and 3F,** Supplemental Figure 4B). Other RV function markers were comparable between the 2 groups (Supplemental Figures 4A and 4B). There was no difference in RV systolic pressure between the 2 groups, indicating that the 2 groups had a similar extent of RV pressure overload (**Figure 3F**). LIPUS therapy significantly ameliorated myocardial hypertrophy and interstitial fibrosis compared with the PAB-placebo group (**Figures 4A and 4B**). In contrast, there was no difference in capillary density between the 2 PAB groups (Supplemental Figures 5A and 5B).

LIPUS THERAPY ACTIVATES THE eNOS-NO-cGMP-PKG SIGNALING PATHWAY. After LIPUS therapy, the extent of eNOS phosphorylation at Ser1177 was significantly increased in PAB-LIPUS mice compared with PAB-placebo mice (**Figures 4C and 4D**), whereas that at Thr495 and the expression of PKC were comparable between the 2 groups (Supplemental Figures 5C and 5D). Furthermore, LIPUS therapy

FIGURE 1 Continued

(A) Representative images of right ventricular myocardial tissues stained for eNOS and caveolin-1 (scale bars: 100 μm for both). **(B)** Quantitative analysis of the positive area of eNOS and caveolin-1. **(C)** Graphs showing the correlation between the positive area of caveolin-1 and eNOS. **(D)** Graphs showing the correlation between the positive area of eNOS and TAPSE, RVFAC, RVSP, mPAP, PCWP, and LVEF. Results are expressed as mean ± SD. *$P < 0.05$. Comparisons of parameters were performed with analysis of variance followed by Tukey's post hoc test for multiple pairwise comparisons. Pearson's correlation coefficient was used to determine the association between 2 continuous variables. Cav-1 = caveolin-1; DCM = dilated cardiomyopathy; eNOS = endothelial nitric oxide synthase; mPAP = mean pulmonary arterial pressure; PAH = pulmonary arterial hypertension; PCWP = pulmonary artery wedge pressure; RVF = right ventricular failure; RVFAC = right ventricular fractional area change; RVSP = right ventricular systolic pressure; TAPSE = tricuspid annular plane systolic excursion.

FIGURE 2 **eNOS Plays a Crucial Role in Mice With Pulmonary Artery Banding**

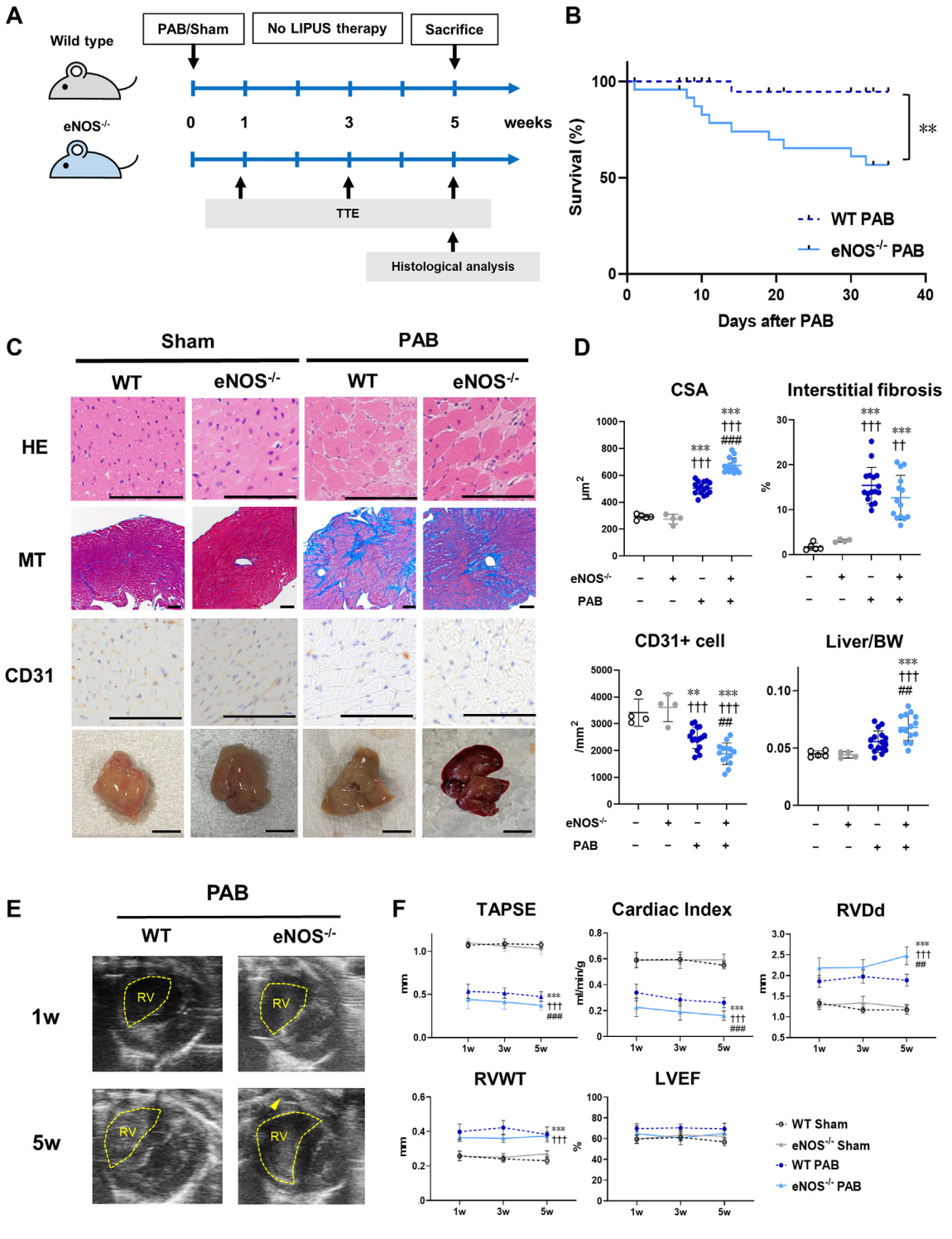

Continued on the next page

significantly upregulated the expression levels of downstream molecules, such as sGCα and PKG Iα in PAB mice (**Figures 4C and 4D**). These results suggest that LIPUS therapy improves RV functions via activating the eNOS-NO-cGMP-PKG signaling pathway. Then, we examined the upstream molecules that are known to phosphorylate eNOS at Ser1177.[29] Phosphorylation of Akt was significantly increased in PAB-LIPUS mice compared with PAB-placebo mice (**Figures 4C and 4D**), whereas phosphorylation of adenosine monophosphate-activated protein kinase (AMPK) and expression of Ca^{2+}/calmodulin-dependent protein kinase II (CaMKII) were comparable between the 2 groups (Supplemental Figures 5C and 5D). Consistently, we found a positive correlation between the extent of phosphorylated eNOS at Ser1177 and sGCα, PKGIα, and phosphorylated Akt (**Figure 4E**), whereas there was no correlation between the extent of phosphorylated eNOS at Ser1177 and phosphorylated AMPK, total AMPK, or CaMKII (Supplemental Figure 5E). The extent of Akt phosphorylation was comparable between sham-operated mice and placebo treatment mice (Supplemental Figures 5F and 5G). In addition, we performed indirect measurement of NO by measuring NO_x (NO_2 + NO_3) levels in the myocardium. Although PAB mice showed lower levels of NO_x compared with WT mice, there was no significant difference between PAB-placebo and PAB-LIPUS mice (Supplemental Figure 6A). Then, we measured cGMP levels in myocardial tissue. Interestingly, myocardial cGMP levels were significantly increased in PAB mice compared with WT mice, and there was no significant difference between PAB-placebo and PAB-LIPUS mice (Supplemental Figure 6B).

CRUCIAL ROLES OF eNOS IN THE THERAPEUTIC EFFECTS OF THE LIPUS THERAPY. To confirm the role of eNOS in the beneficial effects of LIPUS therapy on RVF, we examined the effects of LIPUS therapy in $eNOS^{-/-}$ mice with PAB (**Figure 5A**). In $eNOS^{-/-}$ mice with PAB, LIPUS therapy had no effect on survival rate, echocardiography or hemodynamic data, cardiomyocyte hypertrophy, interstitial fibrosis, or capillary density (**Figures 5B to 5F**). Furthermore, the effects of LIPUS on the downstream molecules of the eNOS-NO-cGMP-PKG signaling pathway were absent in $eNOS^{-/-}$ mice (**Figures 5G and 5H**). Thus, eNOS is crucial for the beneficial effects of LIPUS therapy in the PAB model.

THE EFFECTS OF LIPUS THERAPY TO OTHER PARTS OF THE HEART IN PAB MICE. We additionally examined protein expression of the whole LV at 1 week after the PAB procedure with and without LIPUS therapy. Interestingly, the expression of total eNOS was significantly decreased in the LV of PAB mice, but phosphorylation of eNOS and the expression of the downstream signaling molecules were comparable between sham and PAB mice (Supplemental Figures 7A and 7B), and LV systolic function was unaffected after PAB (**Figure 2F**). Because LIPUS therapy was applied to the whole heart, we also examined the protein expression of the whole LV after LIPUS therapy and found no difference in LV function or protein expression levels of the LV (**Figure 3D,** Supplemental Figures 7C and 7D).

LIPUS THERAPY AMELIORATES RV DYSFUNCTION IN SU/HX RATS. To further confirm the beneficial effects of LIPUS therapy on RVF, we next addressed this issue using another rat model with Sugen/hypoxia (Su/Hx)-induced PAH. SU/Hx rats showed a significant reduction in body weight compared with control rats but showed normal blood pressure and heart rate (Supplemental Figures 8A and 8B). In a treadmill exercise test, SU/Hx rats showed significantly reduced exercise tolerance compared with control rats (Supplemental Figure 8C). There was no difference in exercise tolerance after LIPUS therapy (Supplemental Figure 8C). RV and lung weights were greater in SU/Hx rats than in control rats, whereas no significant difference was noted between SU/Hx-

FIGURE 2 Continued

(A) Experimental protocol. **(B)** Kaplan-Meier curve of WT mice and $eNOS^{-/-}$ mice after PAB (**$P < 0.01$, log-rank test). **(C)** Representative images of RV myocardial tissues stained with hematoxylin-eosin (scale bars: 100 μm), Masson's trichrome (scale bars: 100 μm), CD31 (scale bars: 100 μm), and macroscopic image of the liver (scale bars: 1 cm). **(D)** Quantitative analysis of CSA (HE), myocardial fibrosis (MT), CD31-positive cells, and liver weight (WT sham: n = 5; $eNOS^{-/-}$ sham: n = 4; WT PAB: n = 16; $eNOS^{-/-}$ PAB: n = 14). **(E)** Representative echocardiography images of parasternal short-axis view **(upper)** at 1 week and **(lower)** at 5 weeks after PAB. The arrowhead represents pericardial effusion. **(F)** Graphs showing the time course of TAPSE, cardiac index, RVDd, RVWT, and LVEF evaluated with echocardiography. Results are expressed as mean ± SD. Comparisons of parameters were performed with analysis of variance followed by Tukey's post hoc test for multiple pairwise comparisons. *$P < 0.05$, **$P < 0.01$, ***$P < 0.001$ vs WT sham group; $^{\dagger}P < 0.05$, $^{\dagger\dagger}P < 0.01$, $^{\dagger\dagger\dagger}P < 0.001$ vs $eNOS^{-/-}$ sham group $^{\#}P < 0.05$, $^{\#\#}P < 0.01$, $^{\#\#\#}P < 0.001$ vs WT PAB group. BW = body weight; CSA = cross-sectional area; LIPUS = low-intensity pulsed ultrasound; HE = hematoxylin and eosin; LVEF = left ventricular ejection fraction; MT = Masson's trichrome; PAB = pulmonary artery banding; RV = right ventricle; RVDd = right ventricular diastolic diameter; RVWT = right ventricular wall thickness; TAPSE = tricuspid annular plane systolic excursion; TTE = transthoracic echocardiography; w = weeks; WT = wild type; other abbreviations as in **Figure 1**.

FIGURE 3 LIPUS Therapy Ameliorates RV Dysfunction in Mice With PAB

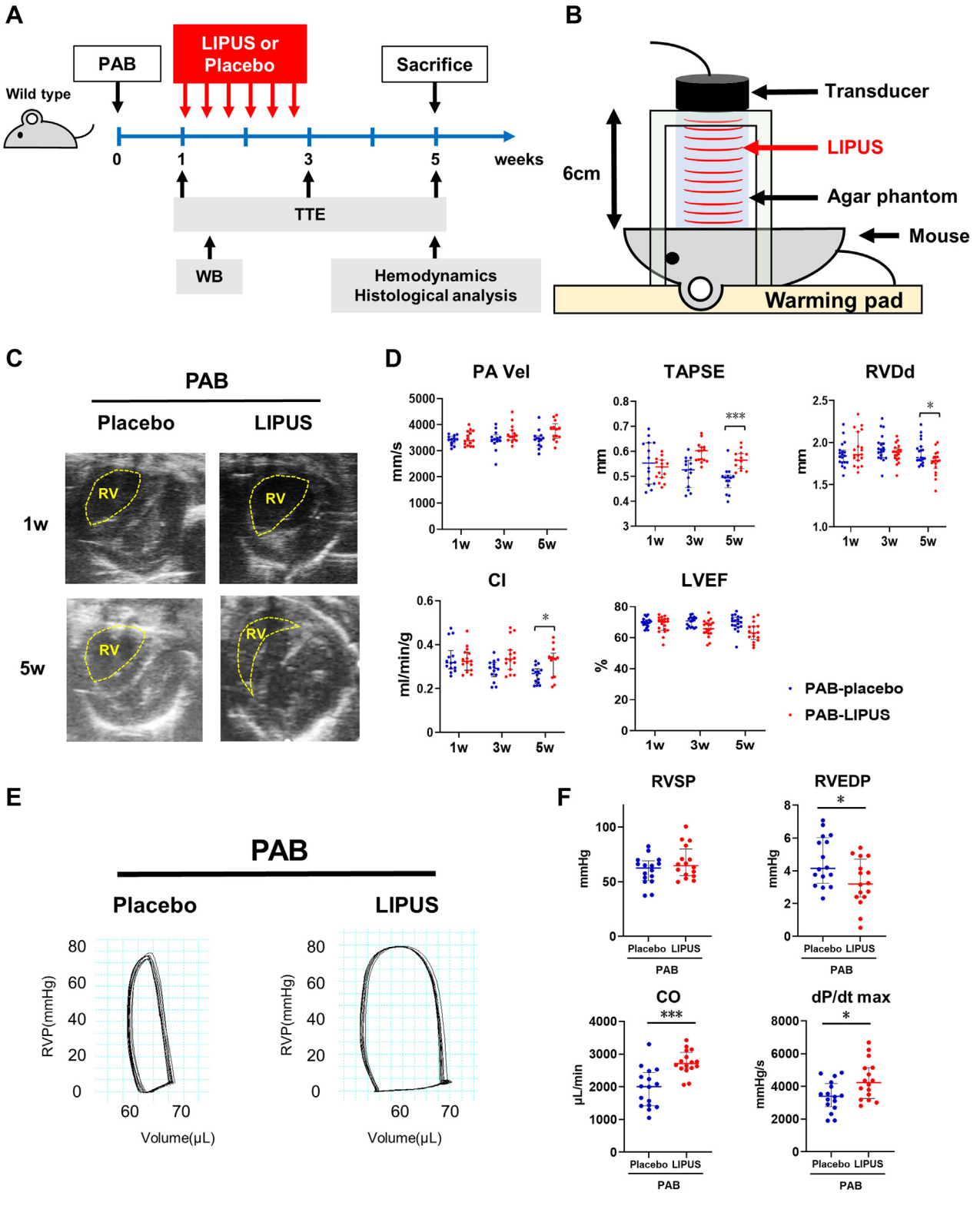

Continued on the next page

placebo and SU/Hx-LIPUS rats (Supplemental Figure 8D). Liver weight was comparable among the 3 groups (Supplemental Figure 8D). There was no significant difference in survival rate between SU/Hx-placebo and SU/Hx-LIPUS rats (Supplemental Figure 8E). Echocardiography examination showed that LIPUS therapy significantly improved TAPSE, right ventricular dilated diameter, CO, and RVFAC (Supplemental Figures 9C, 9D, and 10A). There was no significant difference in LVEF or right ventricular wall thickness between the 2 groups (Supplemental Figure 10A). In the cardiac magnetic resonance (CMR) study, LIPUS therapy significantly ameliorated RV dysfunction in SU/Hx rats, including reduction in right ventricular end diastolic volume and right ventricular end systolic volume and improvement of RVEF (Supplemental Figures 9E and 9F). There was no significant difference in RV mass, left ventricular end diastolic volume and left ventricular end systolic volume, LVEF, or LV mass between SU/Hx-placebo and SU/Hx-LIPUS rats (Supplemental Figure 10B). Invasive hemodynamic evaluation showed that LIPUS therapy significantly improved RV end-diastolic pressure, CO, right ventricular end systolic volume, and RVEF in SU/Hx rats (Supplemental Figures 9G and 9H). In contrast, positive dP/dt and negative dP/dt were unaffected by LIPUS therapy (Supplemental Figure 10C). Importantly, there was no difference in RV systolic pressure, mean pulmonary arterial pressure, pulmonary vascular resistance, or effective arterial elastance between the SU/Hx-placebo and SU/Hx-LIPUS groups, indicating that the severity of pulmonary hypertension was comparable between the 2 groups (Supplemental Figures 9H and 10C). Histologic analysis in SU/Hx rats showed that LIPUS therapy significantly ameliorated cardiomyocyte hypertrophy and interstitial fibrosis compared with the placebo-treated group (Supplemental Figures 11A to 11D). There was no significant difference in capillary density between the SU/Hx-placebo and SU/Hx-LIPUS groups (Supplemental Figures 11E and 11F). Microvascular (<200 μm) vessel occlusion rate in the lung was comparable between the 2 groups (Supplemental Figures 11G and 11H), indicating that LIPUS therapy had no effects on pulmonary vascular occlusion in this SU/Hx model of PAH.

LIPUS THERAPY IMPROVES MYOCARDIAL CA^{2+} HANDLING AND CA^{2+}-RELATED PROTEIN EXPRESSIONS IN SU/HX RATS. To evaluate the effects of LIPUS therapy at the cardiomyocyte level, we examined force and intracellular Ca^{2+} concentration ($[Ca^{2+}]i$) in the trabeculae dissected from the RV during electrical stimulation. There was no difference in developed force between the 2 groups. In the SU/Hx-LIPUS rats, positive peak derivative force (dF/dt max) and negative peak derivative force (dF/dt min) were significantly improved compared with SU/Hx-placebo rats (Supplemental Figures 12A and 12B). Consistently, the trabeculae from the SU/Hx-LIPUS group showed reduced time constant of $[Ca^{2+}]i$ decay compared with SU/Hx-placebo group, whereas there was no significant difference in diastolic $[Ca^{2+}]i$ (Supplemental Figures 12C and 12D). These results indicate that LIPUS therapy ameliorates myocardial systolic and diastolic functions at the cardiomyocyte level. Then, we examined the expressions of Ca^{2+} handling-related molecules in RV tissue. The expression level of phosphorylated phospholamban (PLN) at Ser16 was significantly restored in SU/Hx-LIPUS rats (Supplemental Figures 12E and 12F). In contrast, there was no difference in the expression of total phosphorylated PLN at Thr17 or total PLN among the 3 groups (Supplemental Figures 12E and 12F). Additionally, the expression of sarcoplasmic reticulum Ca^{2+}-ATPase 2a (SERCA2a) was significantly upregulated in the SU/Hx-LIPUS compared with the SU/Hx-placebo group (Figures 12E and 12F). The expression of total eNOS was significantly decreased in the SU/Hx-placebo group and tended to be increased in the SU/Hx-LIPUS group (Supplemental Figures 12E and 12F). Interestingly, we found a positive correlation between total eNOS expression and phosphorylated PLN at Ser16 but not at Thr17 or SERCA2a (Supplemental Figure 12G).

FIGURE 3 Continued

(A) Experimental protocol. **(B)** Schematic drawing showing LIPUS application to a mouse heart. **(C)** Representative echocardiography images of parasternal short-axis view at **(upper)** 1 week and **(lower)** 5 weeks after PAB. **(D)** Graphs showing the time course of PA velocity, TAPSE, RVDd, cardiac index, and LVEF evaluated with echocardiography. ∈ Representative RV pressure-volume loops. **(F)** Graphs showing right ventricular systolic pressure, right ventricular end-diastolic pressure, cardiac output, and dP/dt max evaluated with invasive hemodynamic measurement. Results are expressed as median (IQR). $*P < 0.05$, $**P < 0.01$, $***P < 0.001$. Comparisons of parameters were performed with the Mann-Whitney *U* test. CO = cardiac output; dP/dt = rate of rise of left ventricular pressure; PA Vel = pulmonary arterial velocity; RVEDP = right ventricular end-diastolic pressure; RVP = right ventricular pressure; WB = Western blot; other abbreviations as in **Figures 1 and 2**.

FIGURE 4 LIPUS Therapy Attenuates Cardiomyocyte Hypertrophy and Interstitial Fibrosis and Activates the eNOS-NO-cGMP-PKG Signaling Pathway in Mice With PAB

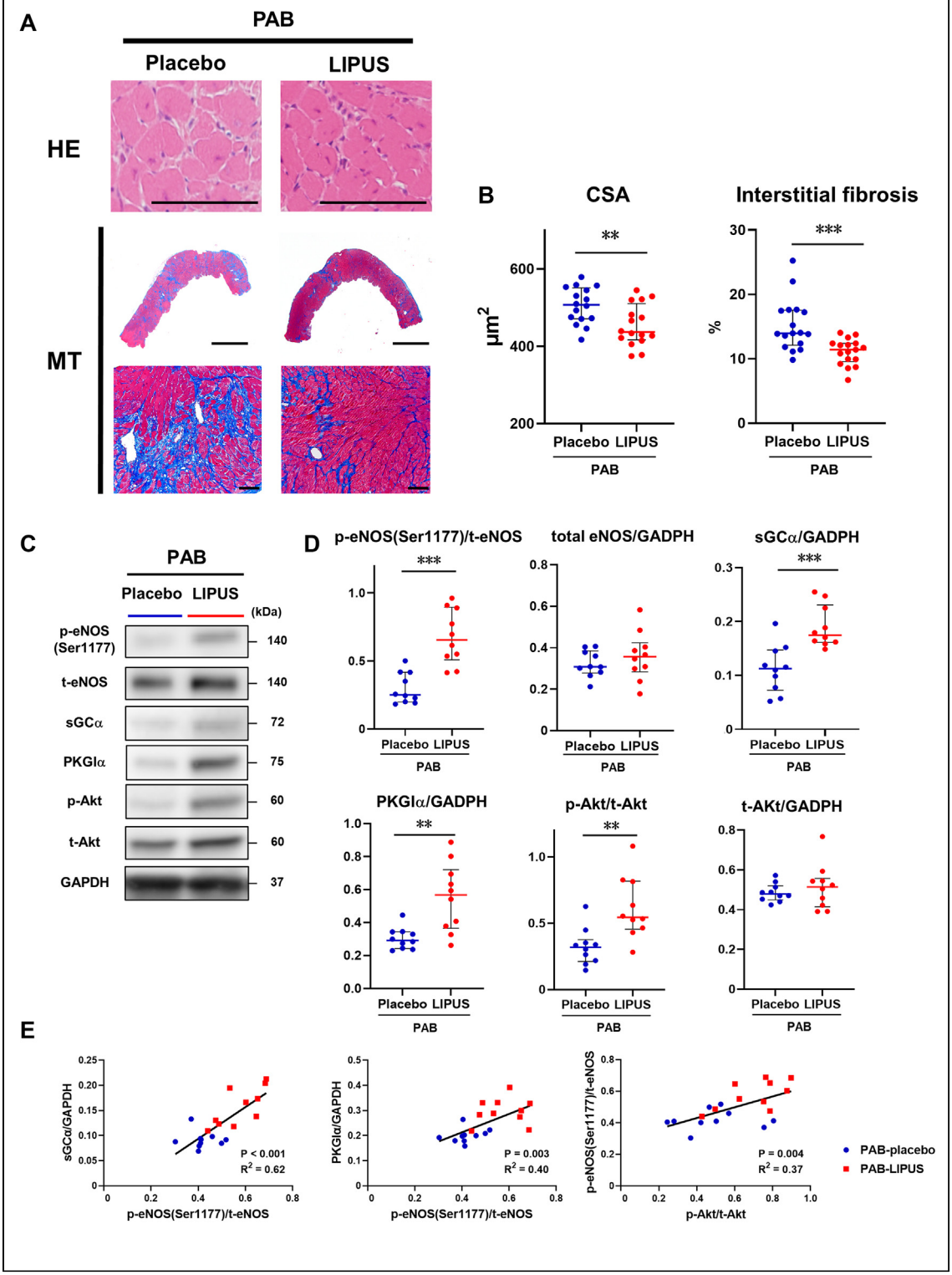

Continued on the next page

DISCUSSION

The major findings of the present study are that: 1) eNOS is downregulated in the RV of patients with RVF caused by dilated cardiomyopathy (DCM) or PAH; 2) impaired eNOS function is substantially involved in the pathogenesis of RVF; 3) LIPUS therapy exerts beneficial effects on RV dysfunction through enhancement of the eNOS-NO-cGMP-PKG pathway in a mouse model of pressure-overloaded RVF (PAB model); and 4) LIPUS therapy ameliorates RV dysfunction and myocardial Ca^{2+} handling without affecting pulmonary arterial lesions in a rat model of PAH (SU/Hx model). To the best of our knowledge, this is the first report demonstrating that LIPUS therapy is effective and safe to improve RV dysfunction in RVF in animals, suggesting that it could be a novel, nonpharmacologic, and less-invasive therapy for patients with PAH.

IMPORTANCE OF eNOS DYSFUNCTION IN THE MECHANISM OF PRESSURE OVERLOAD–INDUCED RV DYSFUNCTION. eNOS plays an important role in the cardiovascular system.[16,17] It has been demonstrated that eNOS and its downstream effectors of the NO-sGC-cGMP-PKG pathway improve cardiac inflammation, hypertrophy, and fibrosis of the LV.[19] However, the protective role of eNOS in pressure-overloaded RV remains to be fully elucidated. In the present study, we confirmed that eNOS is downregulated in the RV of patients with RVF caused by DCM or PAH and SU/Hx rats and that eNOS activity and the NO-sGC-cGMP-PKG pathway were significantly suppressed in PAB mice. There was no statistical difference in the expression of total eNOS in PAB mice. This difference may be explained by the characteristic of this model; the PAB model used in this study was an acute model of RVF. Liao et al[30] reported that the expression of total eNOS in cardiomyocytes was significantly upregulated at the hyperacute phase in the LV pressure overload animal model as a stretch-induced response. They also reported that the expression of total eNOS expression normalized at 1 week after the LV pressure overload. These results indicate that eNOS expression varies depending on the phase of RVF. Taken together, we need further studies to evaluate the time course of eNOS expression, including the hyperacute phase of RV pressure overload. In PAB mice, eNOS suppression may be caused by eNOS phosphorylation at Thr495 as a result of sustained PKC upregulation caused by pressure overload. In addition, $eNOS^{-/-}$ mice with PAB showed worsened pathologic features of RVF compared with WT mice with the same procedure. Thus, sustained suppression of eNOS by phosphorylated PKC at Thr495 and its downstream signaling are highly likely to be involved in the pathogenesis of pressure-overloaded RV dysfunction. In PAB mice, the expression of total eNOS was decreased compared with that in WT mice. This result may be explained by LV diastolic dysfunction induced by compression of enlarged RV.

LIPUS AS A NOVEL THERAPY FOR RVF. Ser1177 is a main phosphorylation site for eNOS activation, which is mediated by several kinases and stimulators.[29] In contrast, eNOS phosphorylation at Thr495 suppresses eNOS activity, for which PKC is involved.[31] PKC is activated in response to pressure overload, sympathetic nerve stimulation, and the renin-angiotensin-aldosterone system.[32] Thus, the RV may be more vulnerable to pressure overload than the LV, resulting in sustained activation of PKC and eNOS phosphorylation at Thr495 in the RV. Because chronic suppression of the eNOS-NO-sGC-cGMP-PKG pathway may have a detrimental effect on RVF, LIPUS therapy could be an effective therapeutic option for this condition, as demonstrated in the present study. In the present study, we also demonstrated that LIPUS therapy improves RV systolic/diastolic functions and Ca^{2+} handling of RV cardiomyocytes in SU/Hx rats. It has been reported that the expression of Ca^{2+}-handling proteins, such as SERCA2a and PLN, were impaired in animal models of PAH[33] and that Ca^{2+}-handling proteins were altered in RV samples from PAH patients undergoing heart-lung

FIGURE 4 Continued

(A) Representative images of myocardial tissues stained with HE (scale bars: 100 μm) and MT (upper scale bars: 1 mm; lower scale bars: 100 μm). **(B)** Quantitative analysis of CSA (HE) and myocardial fibrosis area (MT). **(C, D)** Representative Western blot and quantification of eNOS, phosphorylated eNOS at Ser1177, soluble guanylate cyclase α, protein kinase G Iα, Akt and phosphorylated Akt (p-Akt) in the mouse whole RV. **(E)** Graphs showing the correlation between the expression of phosphorylated eNOS at Ser1177 and sGCα, PKGIα, and phosphorylated Akt. Results are expressed as median (IQR). $*P < 0.05$, $**P < 0.01$, $***P < 0.001$. Comparisons of parameters were performed with the Mann-Whitney *U* test. Pearson's correlation coefficient was used to determine the association between 2 continuous variables. cGMP = cyclic guanosine monophosphate; eNOS = endothelial nitric oxide synthase; GAPDH = glyceraldehyde 3-phosphate dehydrogenase; NO = nitric oxide; p- = phosphorylated; PKG = protein kinase G; PKGIα = protein kinase G Iα; sGCα = soluble guanylate cyclase α; t- = total; other abbreviations as in Figures 1 and 2.

FIGURE 5 No Therapeutic Effects of LIPUS Therapy in eNOS$^{-/-}$ PAB Mice

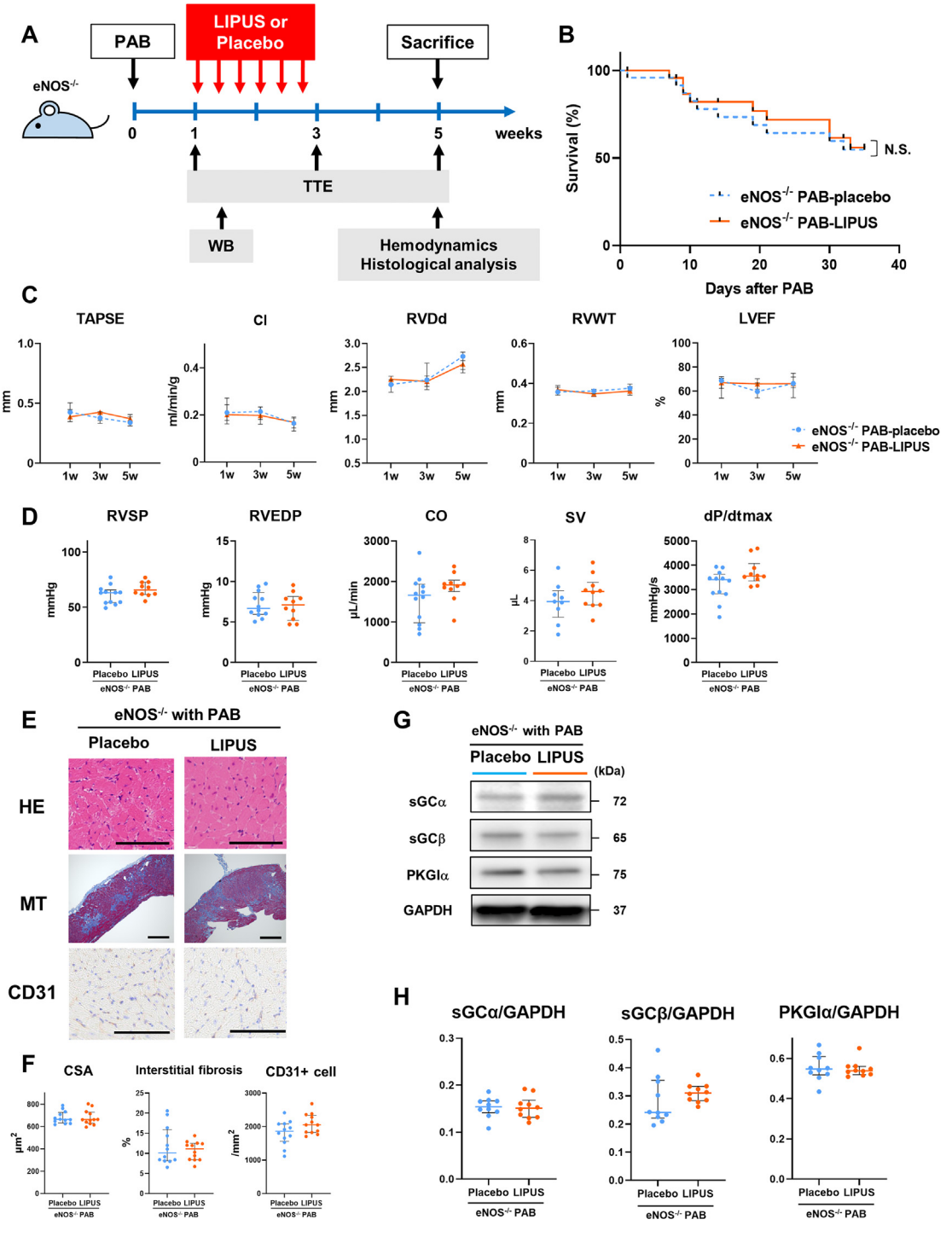

Continued on the next page

transplantation.[34] Although we were unable to demonstrate the acute effects of LIPUS therapy in SU/Hx rats, we demonstrated a positive correlation between the expression of total eNOS and that of phosphorylated PLN at Ser16. Because Ser16 is the major phosphorylation site of PLN activation by PKG,[35] it is possible that LIPUS therapy improves myocardial Ca^{2+} handling through this PKG-mediated PLN activation. Additionally, LIPUS had no effects on the LV (Supplemental Figures 7C and 7D). As we previously reported,[11] LIPUS therapy has no effects on healthy tissue.

LIPUS THERAPY IMPROVES RV FUNCTION IN PAB MICE BY SWITCHING THE PHOSPHORYLATION SITE OF eNOS AND ACTIVATING THE eNOS-NO-sGC-cGMP-PKG PATHWAY. In the present study, we demonstrated that LIPUS therapy improves RV function and ameliorates myocardial hypertrophy and interstitial fibrosis in PAB mice, where the eNOS-sGC-cGMP-PKG pathway plays a crucial role for the therapeutic effects of LIPUS. eNOS is regulated by phosphorylation at multiple sites in response to humoral, mechanical, and pharmacologic stimuli.[16,17] Akt is one of the kinases that phosphorylate eNOS at Ser1177, and the activation of Akt is regulated by tyrosine kinases, G-protein–coupled receptors, and stimulation of cell surface by mechanical forces.[36] We previously reported that LIPUS therapy activates the Akt-eNOS pathway in vivo,[11,12] in which LIPUS-induced mechanical stimulation is involved. AMPK and CaMKII are also known as kinases that phosphorylate eNOS at Ser1177; however, they were not involved in the effects of LIPUS therapy in the present study. Taken together, these results suggest that in RVF with enhanced Thr495 phosphorylation, LIPUS therapy switches the eNOS phosphorylation site from Thr495 to Ser1177 with a resultant enhancement of the eNOS-sGC-cGMP-PKG pathway. Recently, several sGC stimulators have been approved that systemically enhance the sGC-cGMP-PKG pathway[37]; however, eNOS is not involved in their effects. Also, phosphodiesterase (PDE5) inhibitors act through enhancement of cGMP downstream of this pathway. The advantage of LIPUS therapy over these pharmacologic agents is that it is minimally invasive and safe, acting through the suppression of eNOS phosphorylation at Thr495 by enhancing eNOS at Ser1177, the most upstream site of the pathway. To improve the pressure-overloaded condition in RVF, LIPUS therapy is a novel therapeutic approach because it enhances the eNOS-sGC-cGMP-PKG pathway by controlling the activity of eNOS. Although we demonstrated eNOS activation after LIPUS therapy, we were unable to directly show the increase in NO production. Additionally, intracellular cGMP levels were significantly increased in the cardiomyocytes of PAB mice compared with sham-operated mice (Supplemental Figures 6A and 6B). Consistently, protein expression of PDE5 was significantly decreased in the RV of PAB mice compared with sham-operated mice (Supplemental Figures 1D and 1E). These results may have some discrepancies, which may be explained as a compensatory response in the acute phase. In the present study, we were able to measure myocardial cGMP and PDE5 levels only in the acute phase of RVF. We need to evaluate myocardial cGMP levels in other phases of RVF and those in other sources (eg, the serum). Further studies are needed to elucidate other possible mechanisms involved in the therapeutic effects of LIPUS therapy for RVF.

STUDY LIMITATIONS. First, in the present study, we showed the decreased expression of eNOS in RVF patients, but we were unable to show the localization of eNOS because myocardial biopsy samples were fixed only with formalin. Second, we compared the expression of eNOS between DCM patients and PAH patients. Although a comparison of PAH patients with and without RVF would be ideal, in clinical practice, myocardial biopsy is not performed in PAH patients without RVF. Third, in the present study, we used the same condition as in the original experiment.[10] Further studies are needed to optimize the condition of LIPUS therapy for RVF. Fourth, in the present study, we used 2 different animal models of RV pressure overload. Because the pathophysiology of each model is different, the detailed mechanisms of the beneficial effects of LIPUS

FIGURE 5 Continued

(A) Experimental protocol. **(B)** Kaplan-Meier curve of $eNOS^{-/-}$ PAB mice with and without LIPUS therapy (log-rank test). **(C)** Graphs showing the time course of TAPSE, cardiac index, RVDd, RVWT, and LVEF evaluated with echocardiography. **(D)** Graphs showing RVSP, RVEDP, CO, SV, and dP/dt max evaluated with invasive hemodynamic measurement. **(E)** Representative images of myocardial tissues stained with HE (scale bars: 100 μm), MT (scale bars: 500 μm), and CD31 (scale bars: 100 μm). **(F)** Quantitative analysis of CSA (HE), myocardial fibrosis area (MT), and CD31-positive cells. **(G, H)** Representative Western blot and quantification of (sGCα, soluble guanylate cyclase β (sGCβ), and PKGIα) in the mouse whole RV. Results are expressed as median (IQR). SV = stroke volume; other abbreviations as in Figures 1 to 4.

therapy remain to be fully elucidated. In SU/Hx rats, because the acute phase evaluation of the LIPUS therapy was not performed, we were unable to show the activation of eNOS and its downstream signals after LIPUS therapy. However, there was a positive correlation between total eNOS and phosphorylated PLN at Ser16 and between total eNOS and SERCA2a (Supplemental Figure 12G), which suggests that LIPUS-induced eNOS upregulation was involved in the improvement of RV function in SU/Hx rats via restoring the Ca^{2+}-handling system. Additionally, it was reported that the eNOS-NO-sGC-cGMP-PKG pathway possibly activates the Ca^{2+}-handling system, and this pathway exerts inhibitory effects on myocardial hypertrophy and fibrosis as well.[35,38] Although the effects of LIPUS therapy on myocardial hypertrophy and fibrosis were relatively small in the present study, LIPUS therapy seems to significantly enhance the Ca^{2+}-handling system. Further studies are needed to elucidate the detailed mechanisms in the beneficial effects of LIPUS therapy. Fifth, the present mouse model with PAB represents a mild pulmonary hypertension model because we used a 25-gauge needle to create pulmonary arterial banding.[26] However, RV function was significantly impaired by the procedure compared with sham-operated mice (Supplemental Figure 1A). Additionally, in PAB mice, the results of invasive hemodynamic analysis were inconsistent with those of echocardiography. In general, pressure volume analysis of the RV in mice is technically difficult because of the complex shape and small size of the RV. For this reason, we obtained the accurate data with CMR in the SU/Hx rat model. Importantly, in SU/Hx rats, the results of pressure volume analysis were consistent with those of CMR (Supplemental Figures 9E and 9F). Sixth, in the present study, we evaluated the extent of RV ischemia by counting capillary density alone. This issue remains to be examined in future studies. Seventh, although it has been reported that inflammation is involved in the pathophysiology of PAH and RVF,[39] we did not examine inflammation-related factors in the present study. The anti-inflammatory effects of LIPUS therapy remain to be examined in future studies.

CONCLUSIONS

In the present study, we were able to demonstrate that LIPUS therapy ameliorates RVF through activating the eNOS-NO-cGMP-PKG pathway in PAB mice and improved the cardiomyocyte Ca^{2+}-handling system in SU/Hx rats without any adverse effects. The present results indicate that LIPUS therapy could be a novel, nonpharmacologic, and less-invasive therapy strategy for the treatment of patients with PAH.

ACKNOWLEDGMENTS The authors appreciate Y. Watanabe, H. Yamashita, and H. Nonaka for their excellent technical support.

FUNDING SUPPORT AND AUTHOR DISCLOSURES

This research was supported in part by the Japan Agency for Medical Research and Development (grant nos. JP19lm0203047 and JP19lk1403011). The authors have reported that they have no relationships relevant to the contents of this paper to disclose.

ADDRESS FOR CORRESPONDENCE: Dr Hiroaki Shimokawa, International University of Health and Welfare, Narita 286-8686, Japan. E-mail: shimo@iuhw.ac.jp.

PERSPECTIVES

COMPETENCY IN MEDICAL KNOWLEDGE: Although RVF is a major cause of death in pulmonary hypertension patients, no effective treatment is yet available. In this study, we demonstrated that eNOS downregulation is involved in the pathophysiology of RVF and that LIPUS therapy ameliorates RV function through activating eNOS.

TRANSLATIONAL OUTLOOK: LIPUS therapy, which is a noninvasive therapeutic application, could be a promising strategy for RVF patients through eNOS activation without systemic side effects. Because LIPUS therapy could locally activate eNOS in the heart, it could be used as an additional option for RVF patients in addition to established medical treatment.

REFERENCES

1. Arrigo M, Huber LC, Winnik S, et al. Right ventricular failure: pathophysiology, diagnosis and treatment. *Card Fail Rev*. 2019;5:140–146.
2. Weatherald J, Boucly A, Chemla D, et al. Prognostic value of follow-up hemodynamic variables after initial management in pulmonary arterial hypertension. *Circulation*. 2018;137:693–704.
3. Galiè N, Humbert M, Vachiery JL, et al. 2015 ESC/ERS guidelines for the diagnosis and treatment of pulmonary hypertension: the Joint Task Force for the Diagnosis and Treatment of Pulmonary Hypertension of the European Society of Cardiology (ESC) and the European Respiratory Society (ERS): endorsed by: Association for European Paediatric and Congenital Cardiology (AEPC), International Society for Heart and Lung Transplantation (ISHLT). *Eur Heart J*. 2016;37:67–119.
4. Courand PY, Pina Jomir G, Khouatra C, et al. Prognostic value of right ventricular ejection fraction in pulmonary arterial hypertension. *Eur Respir J*. 2015;45:139–149.

5. van de Veerdonk MC, Kind T, Marcus JT, et al. Progressive right ventricular dysfunction in patients with pulmonary arterial hypertension responding to therapy. *J Am Coll Cardiol*. 2011;58:2511–2519.

6. Melenovsky V, Hwang SJ, Lin G, Redfield MM, Borlaug BA. Right heart dysfunction in heart failure with preserved ejection fraction. *Eur Heart J*. 2014;35:3452–3462.

7. Feldman D, Pamboukian SV, Teuteberg JJ, et al. The 2013 International Society for Heart and Lung Transplantation Guidelines for mechanical circulatory support: executive summary. *J Heart Lung Transplant*. 2013;32:157–187.

8. Ryan JJ, Archer SL. The right ventricle in pulmonary arterial hypertension: disorders of metabolism, angiogenesis and adrenergic signaling in right ventricular failure. *Circ Res*. 2014;115:176–188.

9. Shindo T, Shimokawa H. Therapeutic angiogenesis with sound waves. *Ann Vasc Dis*. 2020;13:116–125.

10. Hanawa K, Ito K, Aizawa K, et al. Low-intensity pulsed ultrasound induces angiogenesis and ameliorates left ventricular dysfunction in a porcine model of chronic myocardial ischemia. *PLoS One*. 2014;9:e104863.

11. Shindo T, Ito K, Ogata T, et al. Low-intensity pulsed ultrasound enhances angiogenesis and ameliorates left ventricular dysfunction in a mouse model of acute myocardial infarction. *Arterioscler Thromb Vasc Biol*. 2016;36:1220–1229.

12. Ogata T, Ito K, Shindo T, et al. Low-intensity pulsed ultrasound enhances angiogenesis and ameliorates contractile dysfunction of pressure-overloaded heart in mice. *PLoS One*. 2017;12:e0185555.

13. Monma Y, Shindo T, Eguchi K, et al. Low-intensity pulsed ultrasound ameliorates cardiac diastolic dysfunction in mice. A possible novel therapy for HFpEF. *Cardiovasc Res*. 2021;117:1325–1338.

14. Forstermann U, Sessa WC. Nitric oxide synthases: regulation and function. *Eur Heart J*. 2012;33:829–837.

15. Wallerath T, Gath I, Aulitzky WE, Pollock JS, Kleinert H, Forstermann U. Identification of the NO synthase isoforms expressed in human neutrophil granulocytes, megakaryocytes and platelets. *Thromb Haemostasis*. 1997;77:163–167.

16. Lundberg JO, Gladwin MT, Weitzberg E. Strategies to increase nitric oxide signalling in cardiovascular disease. *Nat Rev Drug Discov*. 2015;14:623–641.

17. Vanhoutte PM, Shimokawa H, Feletou M, Tang EH. Endothelial dysfunction and vascular disease—a 30th anniversary update. *Acta Physiol (Oxf)*. 2017;219:22–96.

18. Farah C, Michel LYM, Balligand J-L. Nitric oxide signalling in cardiovascular health and disease. *Nat Rev Cardiol*. 2018;15:292–316.

19. Emdin M, Aimo A, Castiglione V, et al. Targeting cyclic guanosine monophosphate to treat heart failure. *J Am Coll Cardiol*. 2020;76:1795–1807.

20. Park M, Sandner P, Krieg T. cGMP at the centre of attention: emerging strategies for activating the cardioprotective PKG pathway. *Basic Res Cardiol*. 2018;113:24.

21. Takimoto E, Champion HC, Li M, et al. Chronic inhibition of cyclic GMP phosphodiesterase 5A prevents and reverses cardiac hypertrophy. *Nat Med*. 2005;11:214–222.

22. Nagayama T, Hsu S, Zhang M, et al. Sildenafil stops progressive chamber, cellular, and molecular remodeling and improves calcium handling and function in hearts with pre-existing advanced hypertrophy caused by pressure overload. *J Am Coll Cardiol*. 2009;53:207–215.

23. Nergui S, Fukumoto Y, Zhulanqiqige D, et al. Role of endothelial nitric oxide synthase and collagen metabolism in right ventricular remodeling due to pulmonary hypertension. *Circ J*. 2014;78:1465–1474.

24. Bisserier M, Pradhan N, Hadri L. Current and emerging therapeutic approaches to pulmonary hypertension. *Rev Cardiovasc Med*. 2020;21:163–179.

25. Ichijo S, Shindo T, Eguchi K, et al. Low-intensity pulsed ultrasound therapy promotes recovery from stroke by enhancing angio-neurogenesis in mice in vivo. *Sci Rep*. 2021;11:4958.

26. Rockman HA, Ono S, Ross RS, et al. Molecular and physiological alterations in murine ventricular dysfunction. *Proc Natl Acad Sci U S A*. 1994;91:2694–2698.

27. Abe K, Toba M, Abdallah A, et al. Formation of plexiform lesions in experimental severe pulmonary arterial hypertension. *Circulation*. 2010;121:2747–2754.

28. Edward GS, Maeda N, Kim HS, et al. Elevated blood pressures in mice lacking endothelial nitric oxide synthase. *Proc Natl Acad Sci U S A*. 1996;93:13176–13181.

29. Mount PF, Kemp BE, Power DA. Regulation of endothelial and myocardial NO synthesis by multisite eNOS phosphorylation. *J Mol Cell Cardiol*. 2007;42:271–279.

30. Liao X, Liu JM, Tang A, et al. Nitric oxide signaling in stretch-induced apoptosis of neonatal rat cardiomyocytes. *FASEB J*. 2006;20:1883–1885.

31. Matsubara M, Hayashi N, Jing T, Titani K. Regulation of endothelial nitric oxide synthase by protein kinase C. *J Biochem*. 2003;133:773–781.

32. Ferreira JC, Brum PC, Mochly-Rosen D. βIIPKC and εPKC isozymes as potential pharmacological targets in cardiac hypertrophy and heart failure. *J Mol Cell Cardiol*. 2011;51:479–484.

33. Power AS, Hickey AJ, Crossman DJ, Loiselle DS, Ward ML. Calcium mishandling impairs contraction in right ventricular hypertrophy prior to overt heart failure. *Pflugers Arch*. 2018;470:1115–1126.

34. Rain S, Bos Dda S, Handoko ML, et al. Protein changes contributing to right ventricular cardiomyocyte diastolic dysfunction in pulmonary arterial hypertension. *J Am Heart Assoc*. 2014;3:e000716.

35. Frantz S, Klaiber M, Baba HA, et al. Stress-dependent dilated cardiomyopathy in mice with cardiomyocyte-restricted inactivation of cyclic GMP-dependent protein kinase I. *Eur Heart J*. 2013;34:1233–1244.

36. Fulton D, Gratton JP, McCabe TJ, et al. Regulation of endothelium-derived nitric oxide production by the protein kinase Akt. *Nature*. 1999;399:597–601.

37. Armstrong PW, Pieske B, Anstrom KJ, et al. Vericiguat in patients with heart failure and reduced ejection fraction. *N Engl J Med*. 2020;382:1883–1893.

38. Inserte J, Garcia-Dorado D. The cGMP/PKG pathway as a common mediator of cardioprotection: translatability and mechanism. *Br J Pharmacol*. 2015;172:1996–2009.

39. Dewachter L, Dewachter C. Inflammation in right ventricular failure: does it matter? *Front Physiol*. 2018;9:1056.

KEY WORDS endothelial NO synthase, LIPUS, noninvasive therapy, pulmonary hypertension, right ventricular dysfunction

APPENDIX For a supplemental Methods section as well as a table, figures, and references, please see the online version of this paper.